Supplemental Simulation Case Studies of Dynamic Evaporator Modeling Paradigms with Variable Fluid Phases

Erik Rodriguez[1], Bryan Rasmussen[2]

The purpose of this document is to present a multitude of case studies comparing evaporator modeling techniques for dynamic vapor compression system simulations that can handle the appearance and disappearance of fluid phases in the heat exchanger. Switched moving boundary (SMB) and finite control volume methods are analyzed. Switching approaches include (1) enthalpy based switching which uses two-phase region length and evaporator outlet enthalpy as an event trigger, (2) void fraction based switching which includes the mean void fraction in the state variable vector, and (3) density based switching which uses two-phase region density to trigger mass conservative switching. Nine case studies are performed through a combination of three different refrigerants, three different physical system parameters, and three different operating conditions. Details regarding these case studies are presented in Table I. Output pressures, superheats, and air temperatures are included for comparison. The number of switches triggered during simulation are also presented for comparison. Simulation results were generated using Matlab/Simulink version R2010b on an Intel Core i3 CPU (3.20 GHz) with 8 GB RAM. All systems simulated used dry air as the external fluid and used the heat transfer correlations and numerical simulation details provided in Table II.

[1]PhD candidate in the Department of Mechanical Engineering at Texas A&M University, College Station, TX 77843-3123, USA

[2]Associate Professor in the Department of Mechanical Engineering at Texas A&M University, College Station, TX 77843-3123, USA

TABLE I: Operating Conditions

	Case 1	Case 2	Case 3
Boundary conditions	R-404A	R-410A	R-134a
Mass flow rate (kg/s)	0.020	0.015	0.012
Inlet pressure (kPa)	800	467	250
Inlet enthalpy (kJ/kg)	250	230	300
Boundary conditions (Dry Air)			
Mass flow rate (kg/s)	0.300	0.210	0.157
Inlet temperature (°C)	23	15	15
Physical Parameters			
Hydraulic diameter (m)	1.00×10^{-2}	8.6×10^{-3}	8.10×10^{-3}
Total heat exchanger tube length (m)	20.000	34.490	11.458
Cross-sectional area (m^2)	7.50×10^{-5}	1.16×10^{-4}	5.16×10^{-5}
External surface area (m^2)	3.000	19.154	0.652
Internal surface area (m^2)	0.500	2.059	0.292
Wall mass (kg)	4.000	6.486	2.744
Wall specific heat (kJ/(kg-K))	0.467	0.900	0.488
Input Changes			
Valve Opening	Case 1a	Case 2a	Case 3a
External Fluid Fan Speed	Case 1b	Case 2b	Case 3b
Compressor Speed	Case 1c	Case 2c	Case 3c

TABLE II: Simulation Parameters

Correlations	
Single-phase heat transfer correlation	Gnielinski (1976)
Two-phase heat transfer correlation	Wattlet (1994)
External heat transfer correlation	Kays And London (1984)
Simulation details	
Simulation time (s)	400
Simulation step size (s)	0.01
Solver	Fourth Order Runge-Kutta

A. Length Threshold Analysis

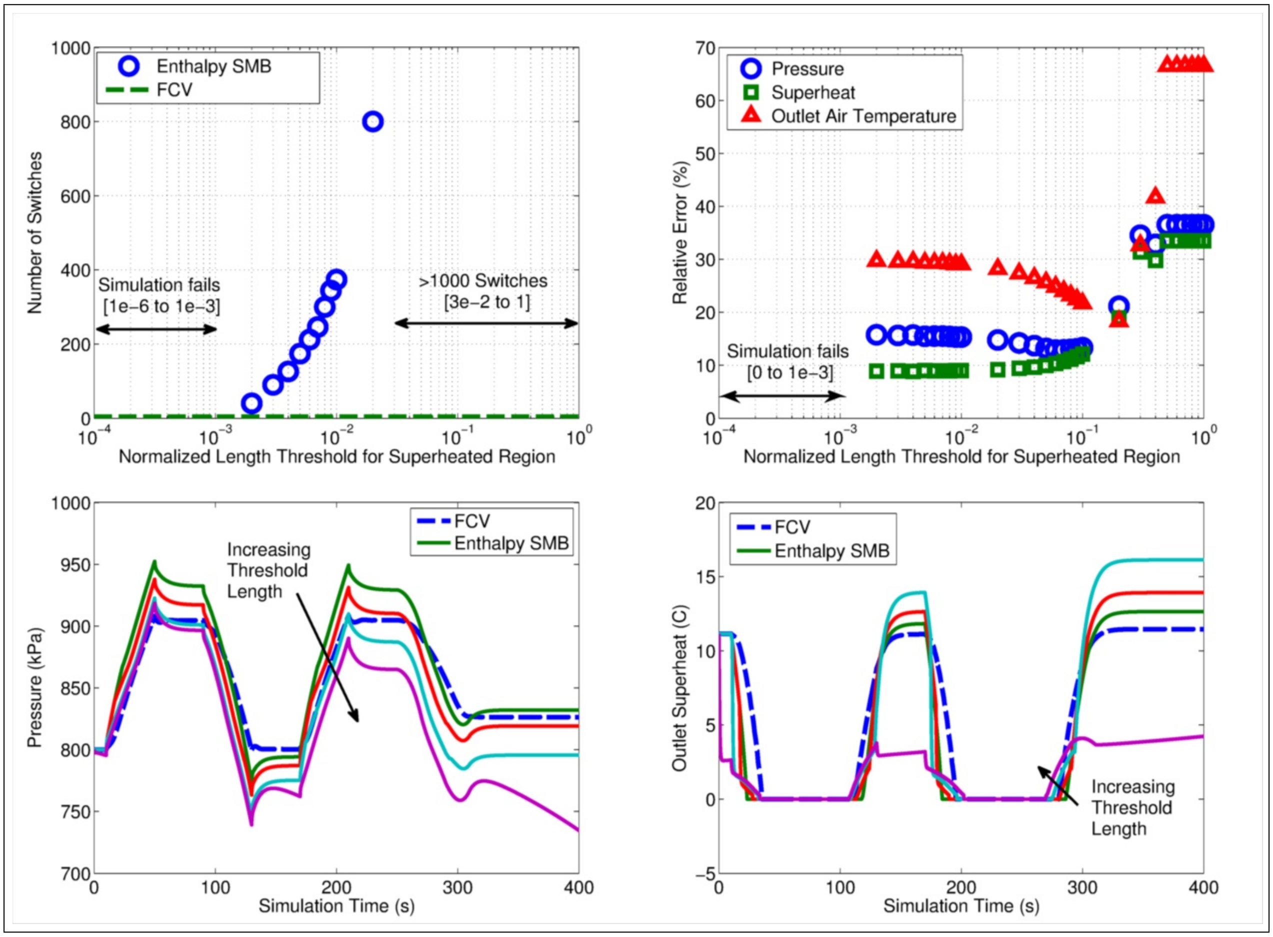

Fig. 1: Comparison of minimum normalized threshold length, l_{eps}, for enthalpy based SMB model - Case 1a

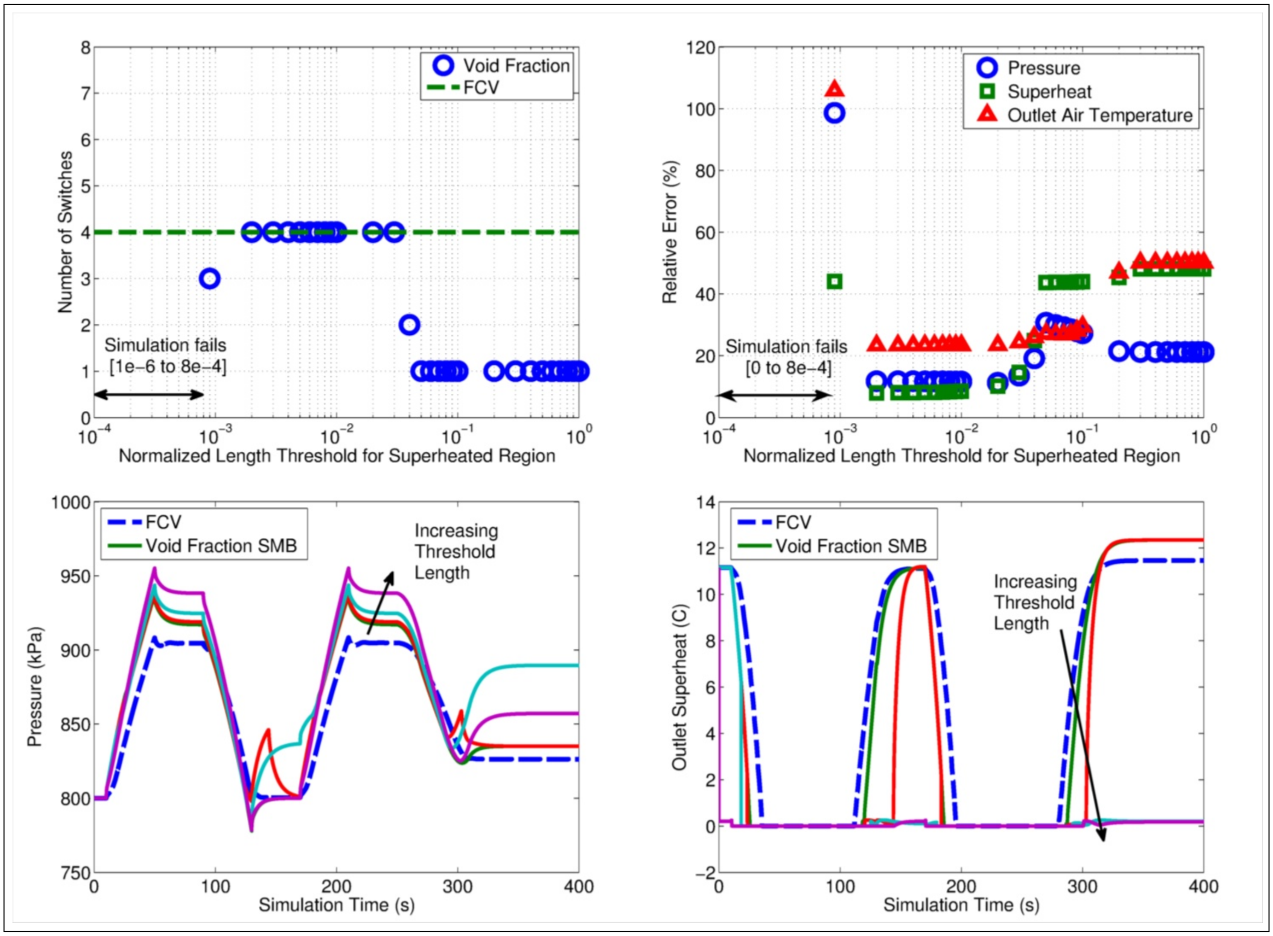

Fig. 2: Comparison of minimum normalized threshold length, l_{eps}, for void fraction based SMB model - Case 1a

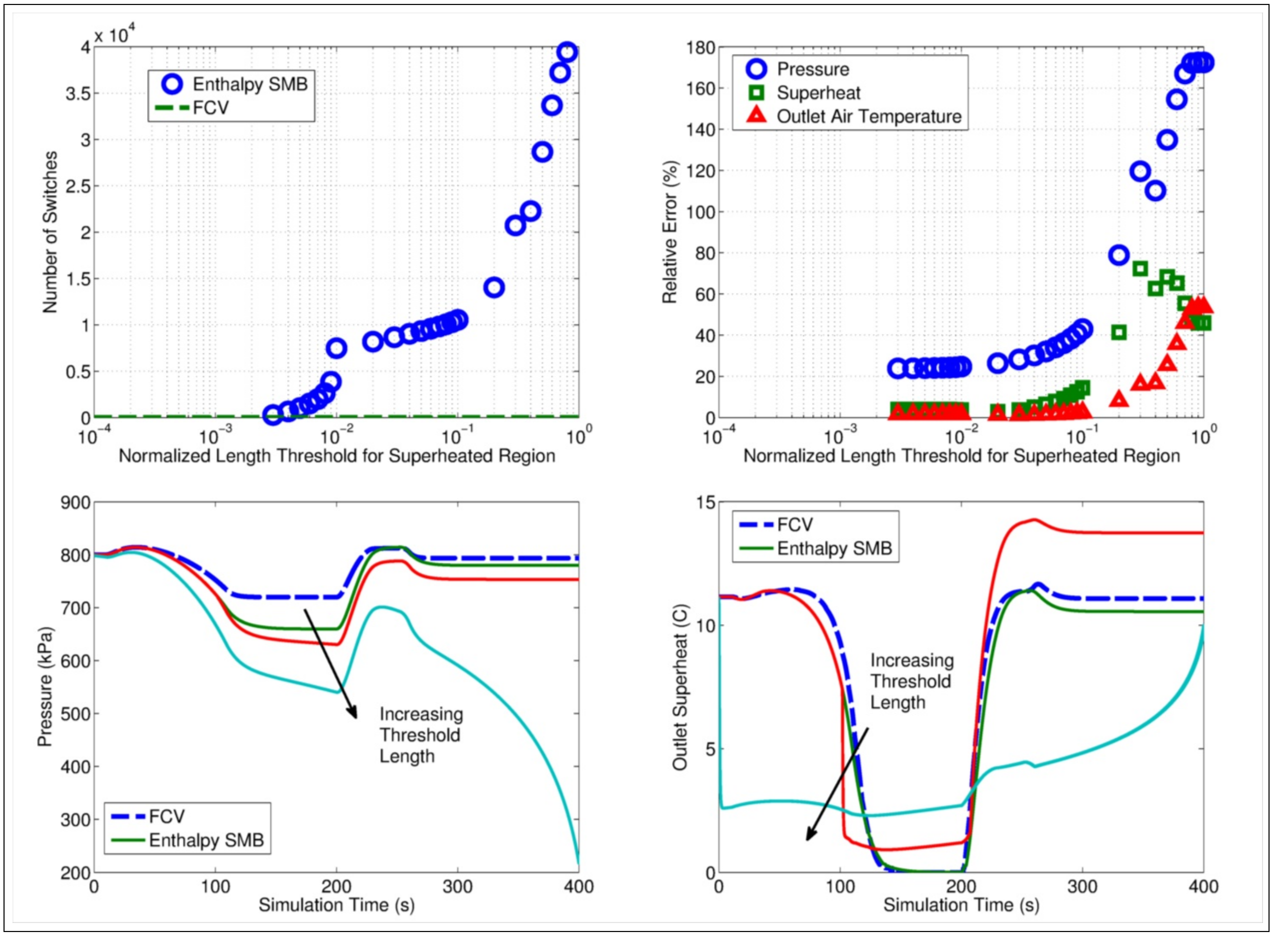

Fig. 3: Comparison of minimum normalized threshold length, l_{eps}, for enthalpy based SMB model - Case 1b

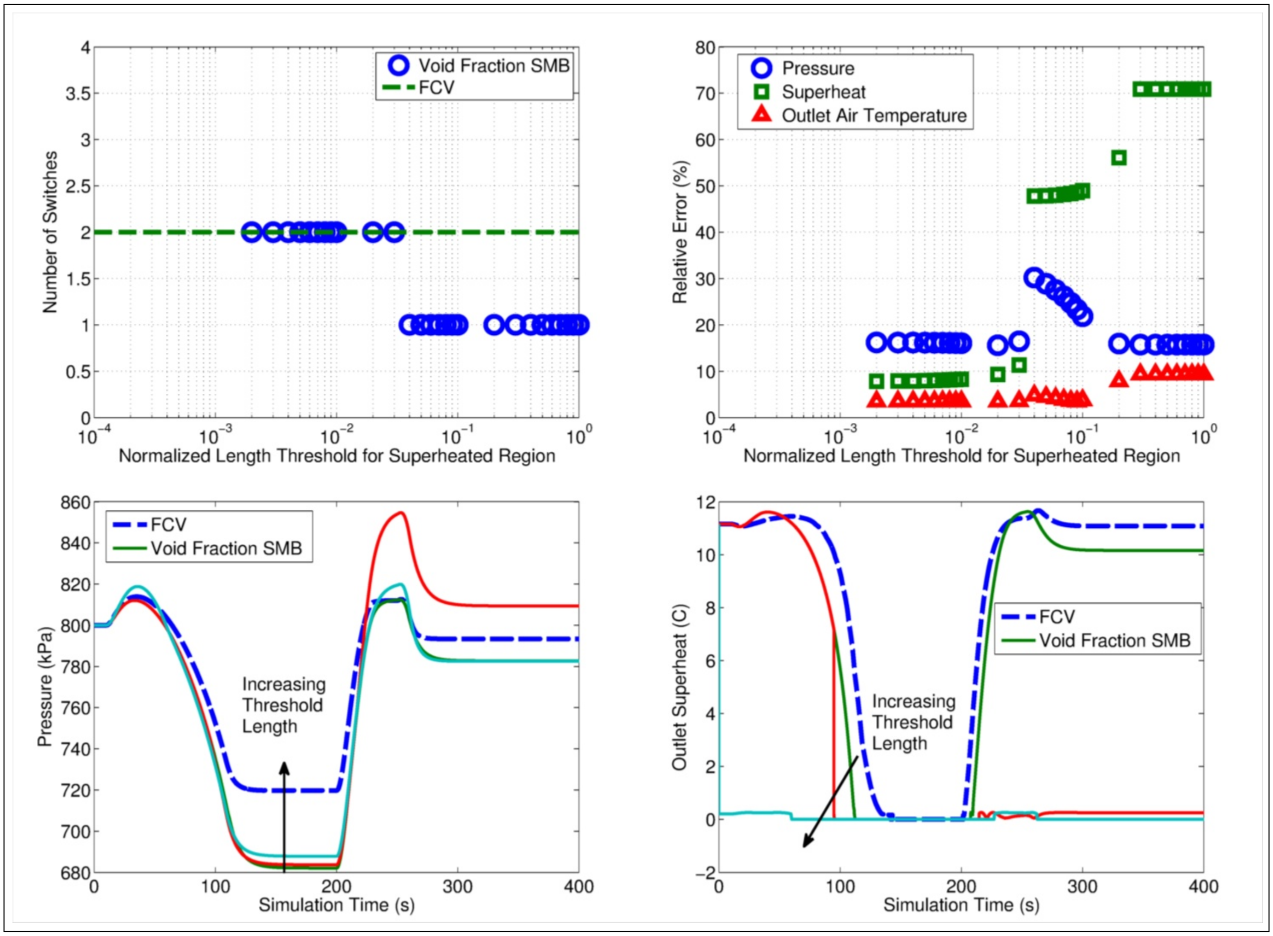

Fig. 4: Comparison of minimum normalized threshold length, l_{eps}, for void fraction based SMB model - Case 1b

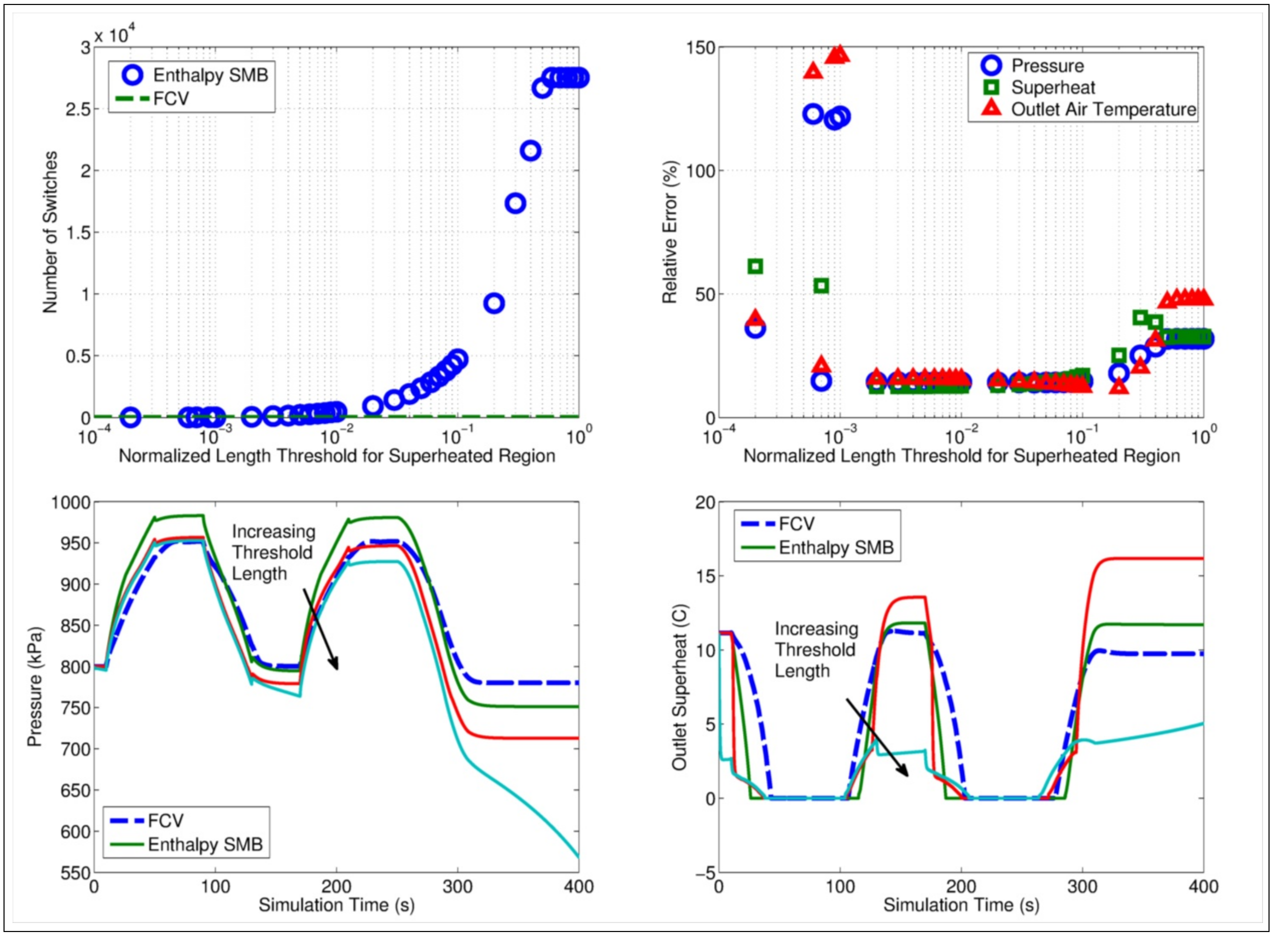

Fig. 5: Comparison of minimum normalized threshold length, l_{eps}, for enthalpy based SMB model - Case 1c

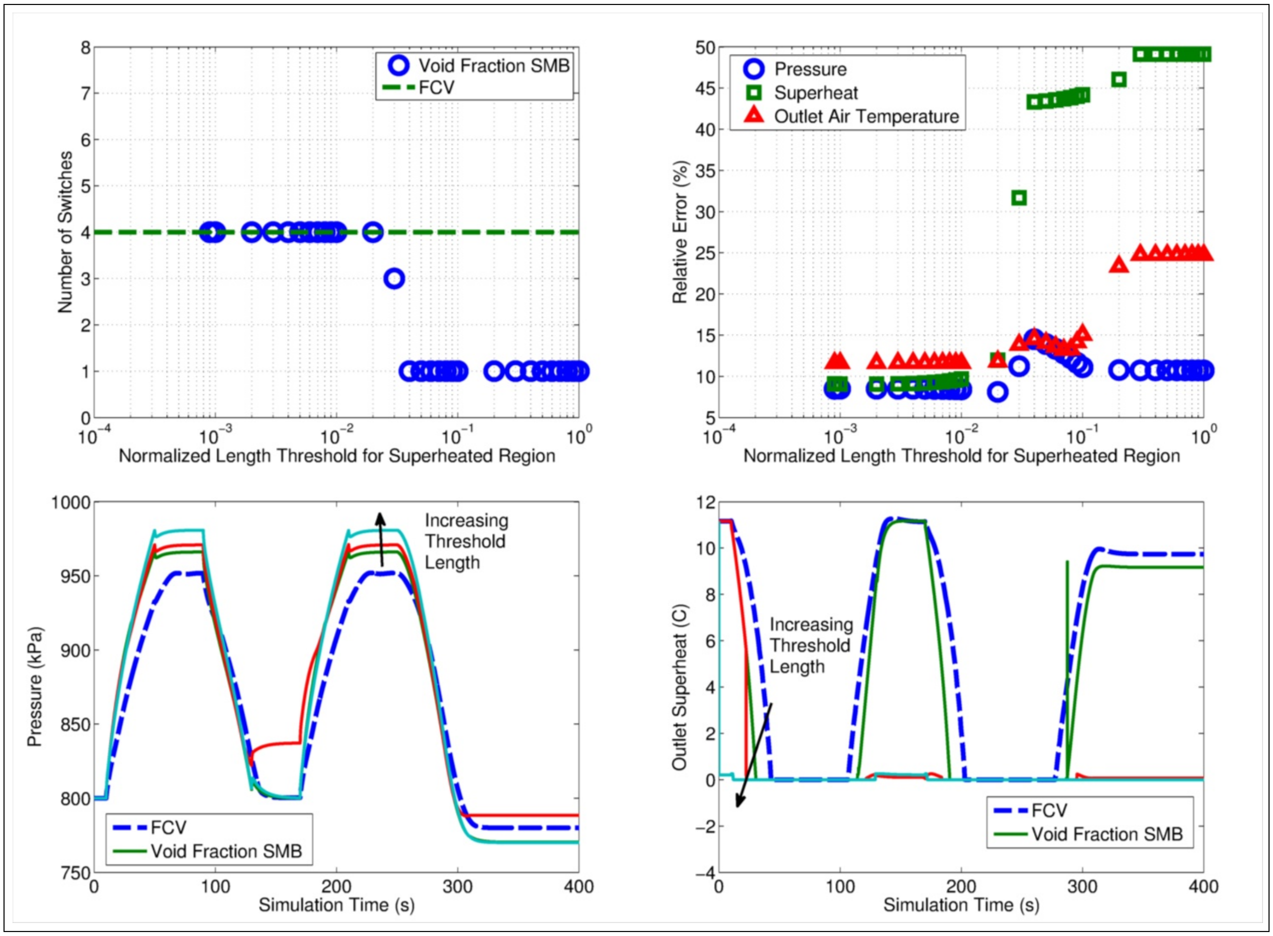

Fig. 6: Comparison of minimum normalized threshold length, l_{eps}, for void fraction based SMB model - Case 1c

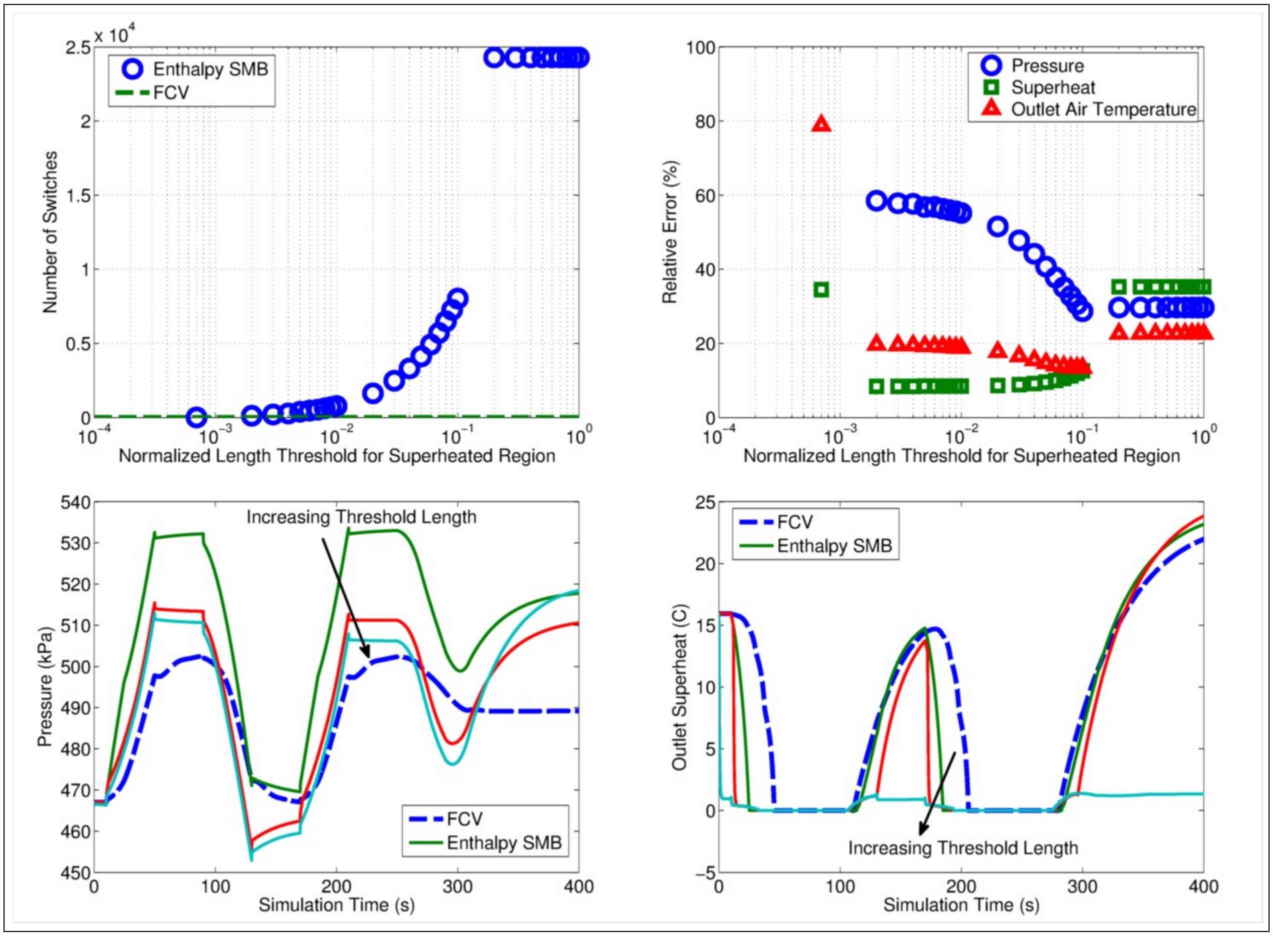

Fig. 7: Comparison of minimum normalized threshold length, l_{eps}, for enthalpy based SMB model - Case 2a

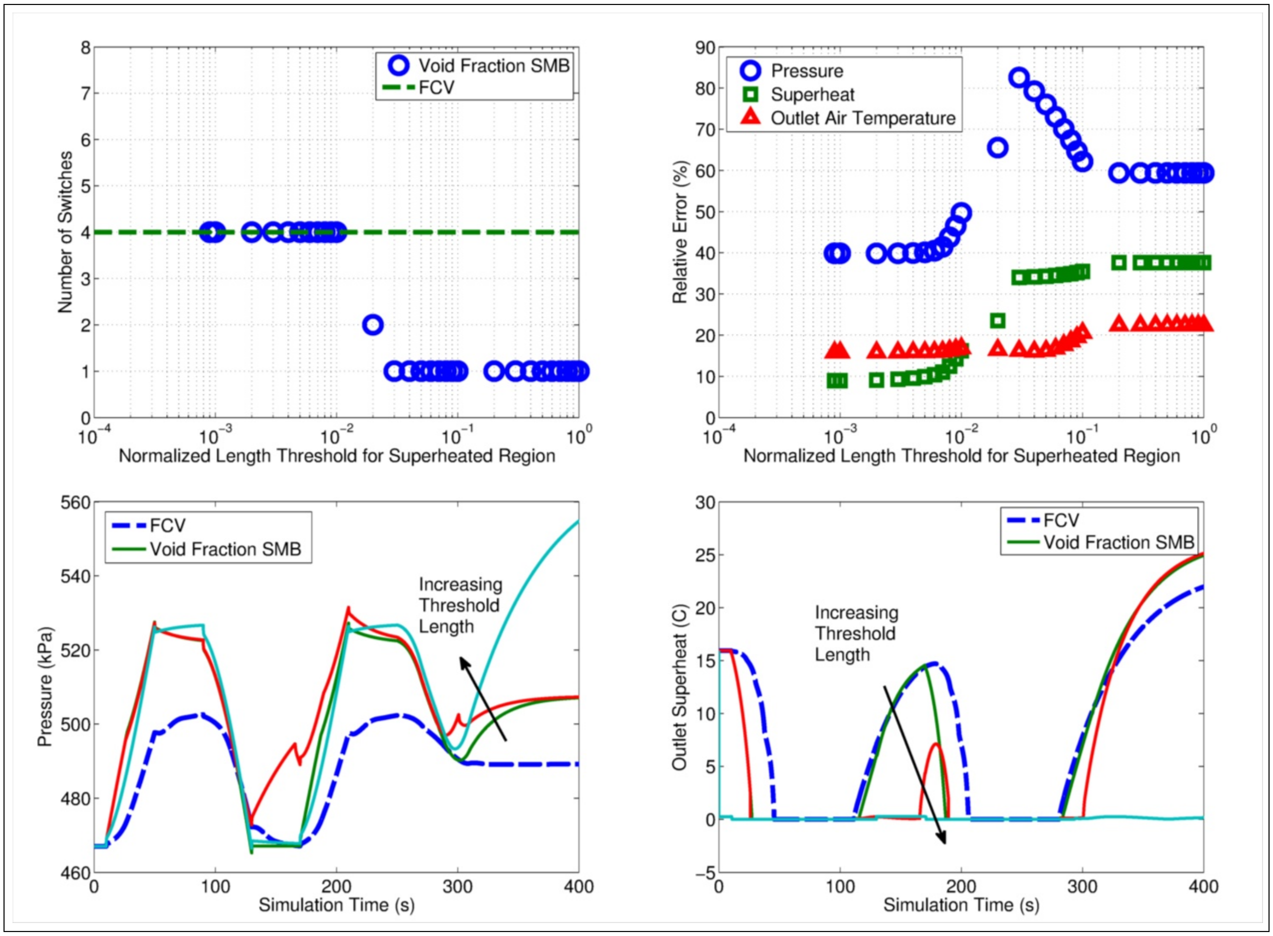

Fig. 8: Comparison of minimum normalized threshold length, l_{eps}, for void fraction based SMB model - Case 2a

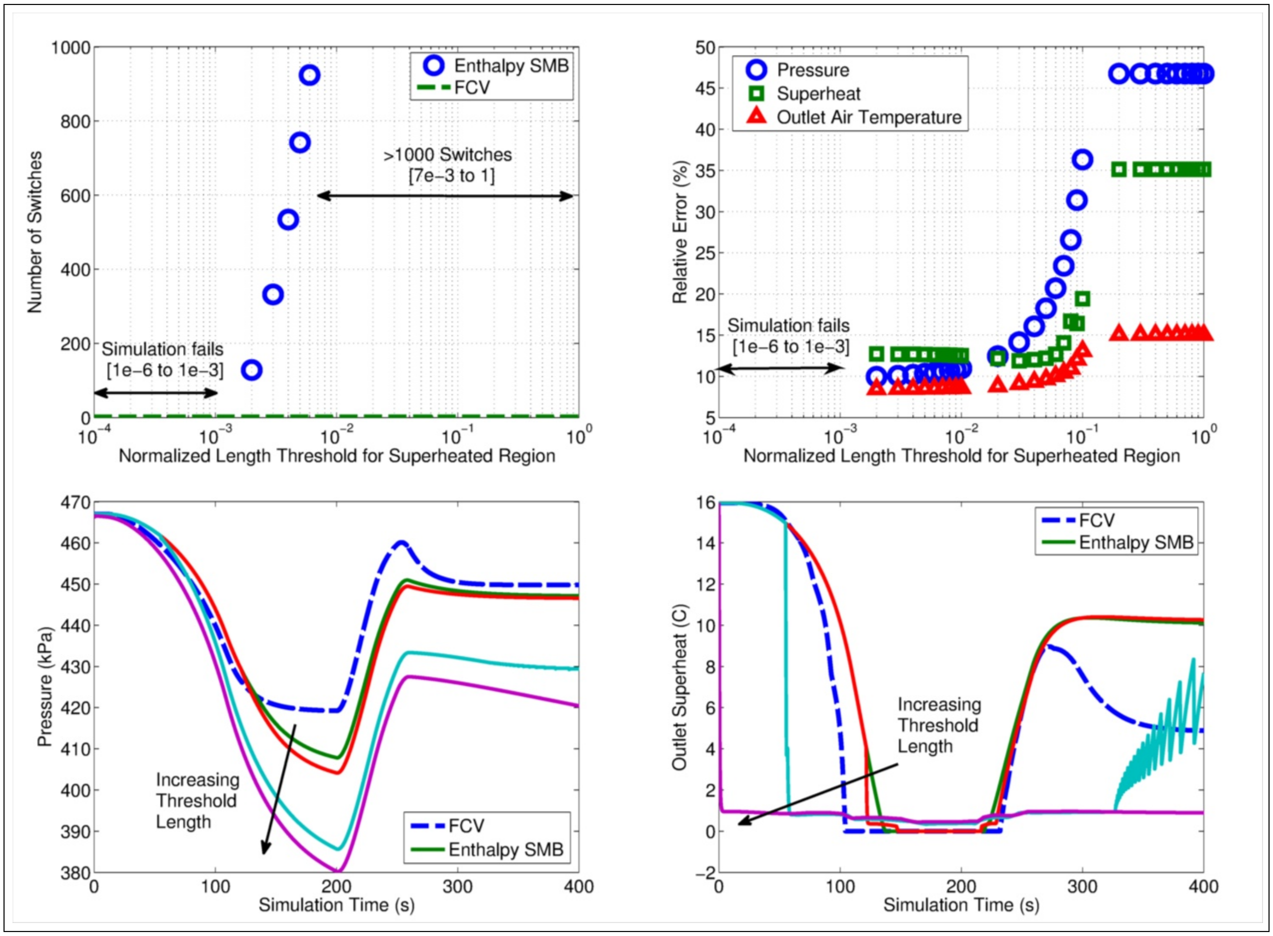

Fig. 9: Comparison of minimum normalized threshold length, l_{eps}, for enthalpy based SMB model - Case 2b

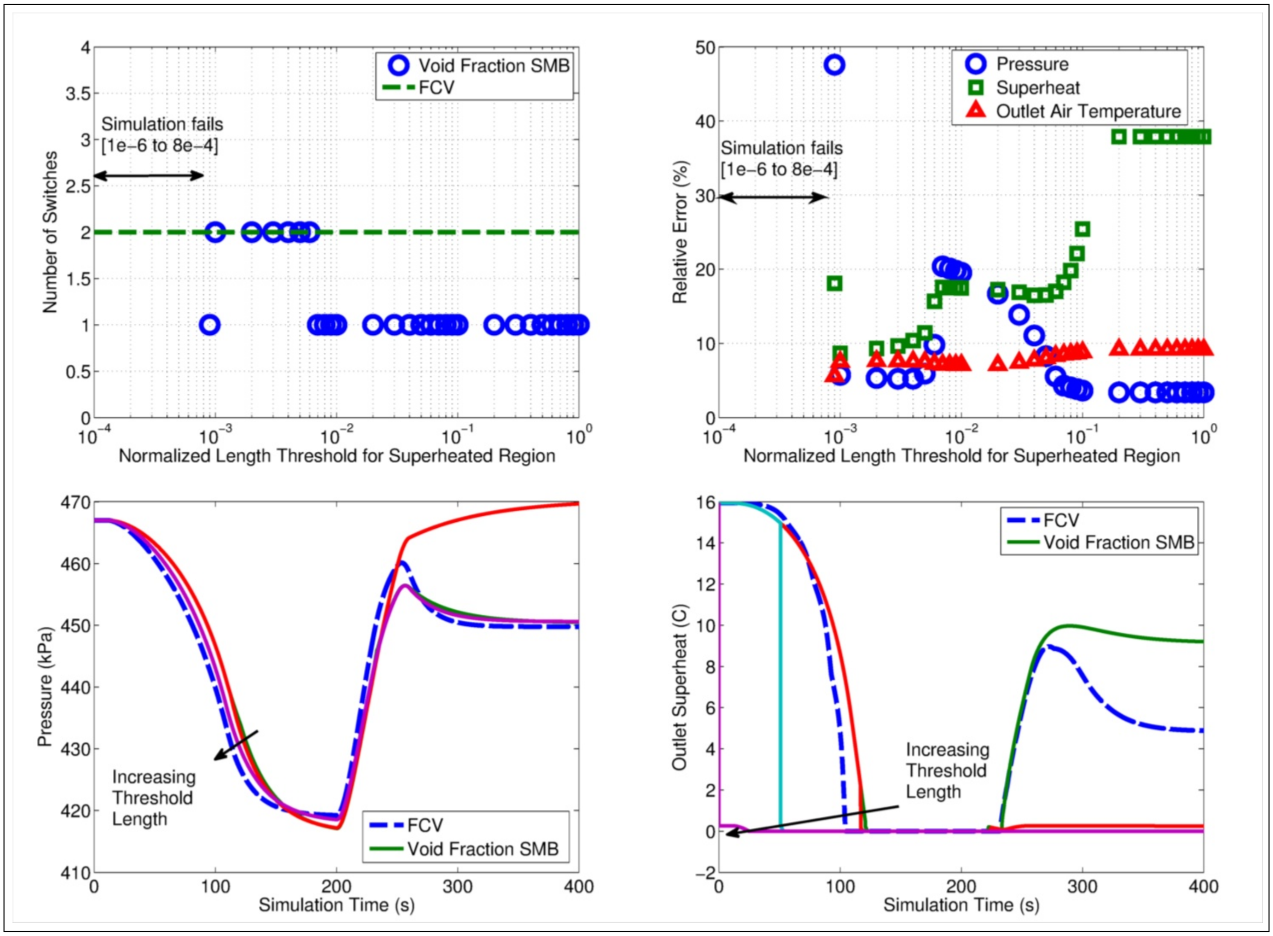

Fig. 10: Comparison of minimum normalized threshold length, l_{eps}, for void fraction based SMB model - Case 2b

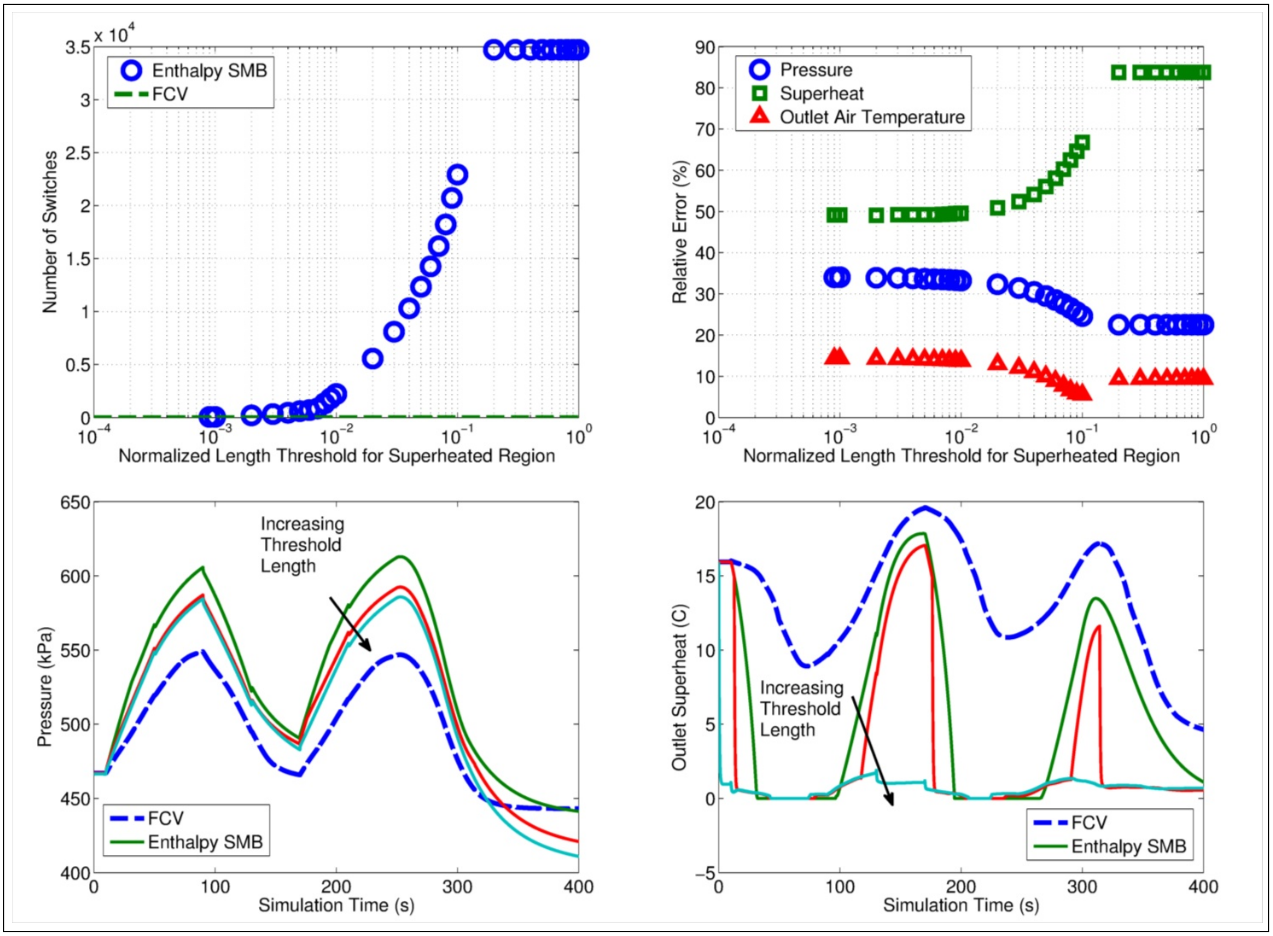

Fig. 11: Comparison of minimum normalized threshold length, l_{eps}, for enthalpy based SMB model - Case 2c

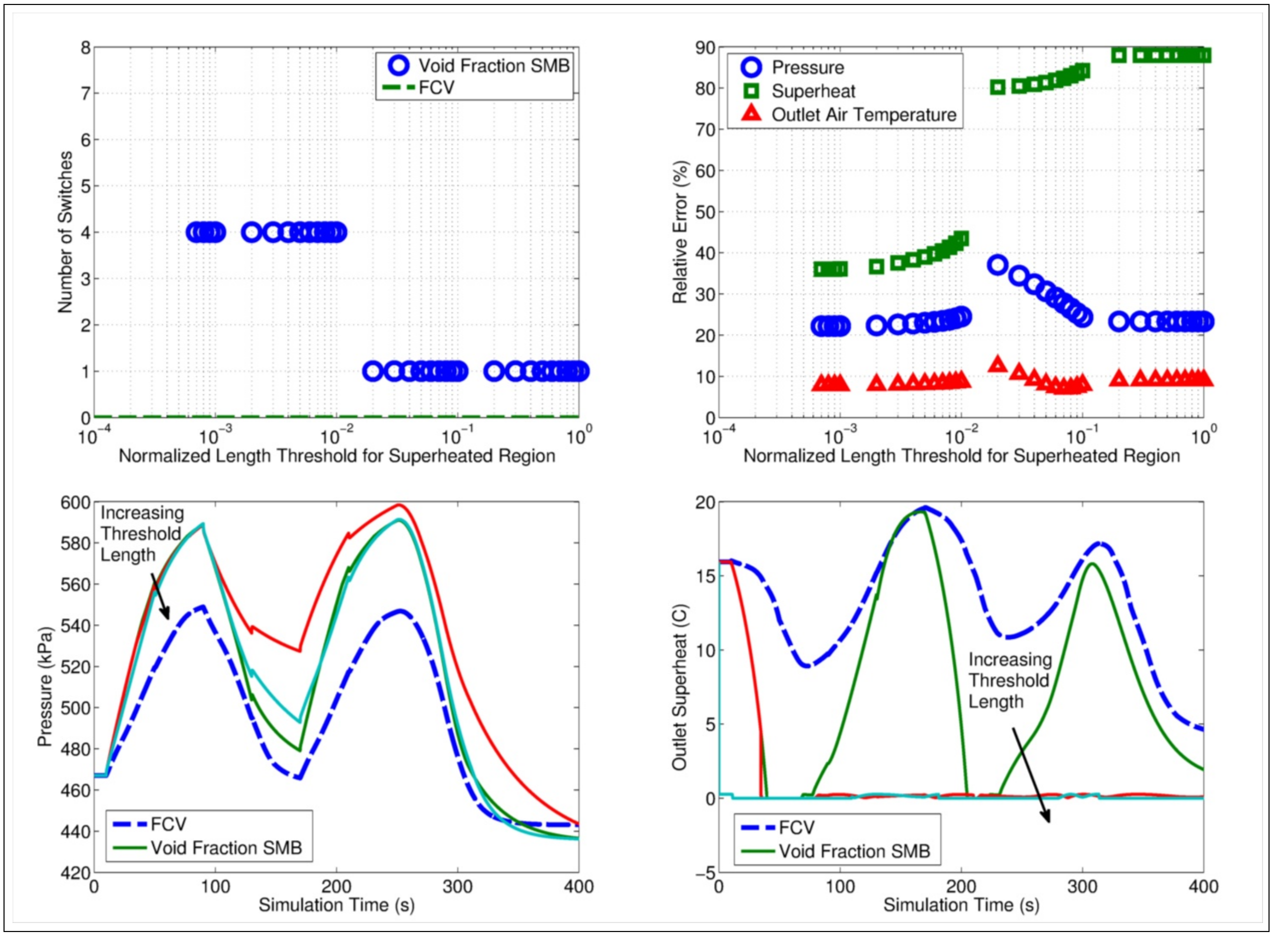

Fig. 12: Comparison of minimum normalized threshold length, l_{eps}, for void fraction based SMB model - Case 2c

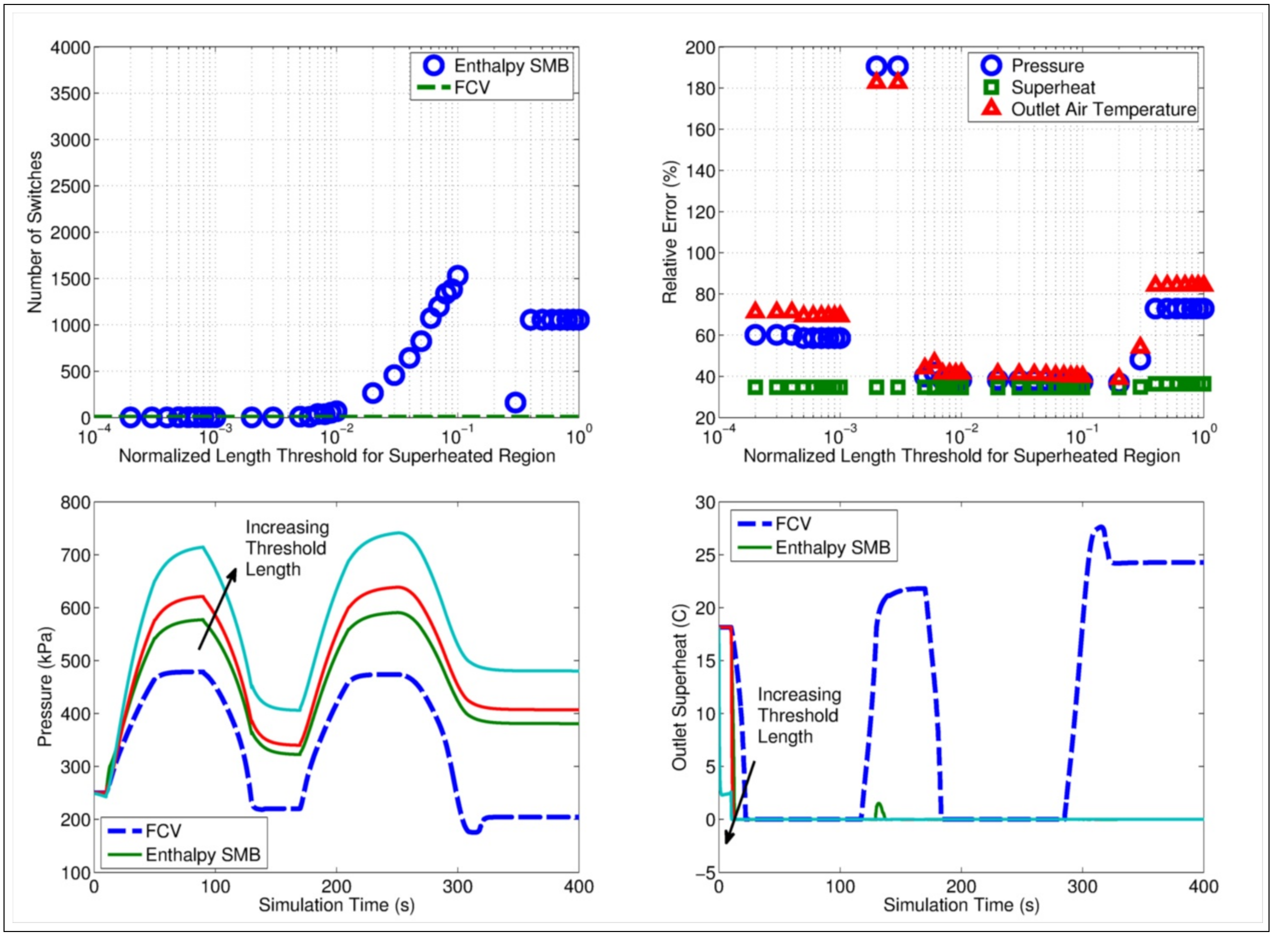

Fig. 13: Comparison of minimum normalized threshold length, l_{eps}, for enthalpy based SMB model - Case 3a

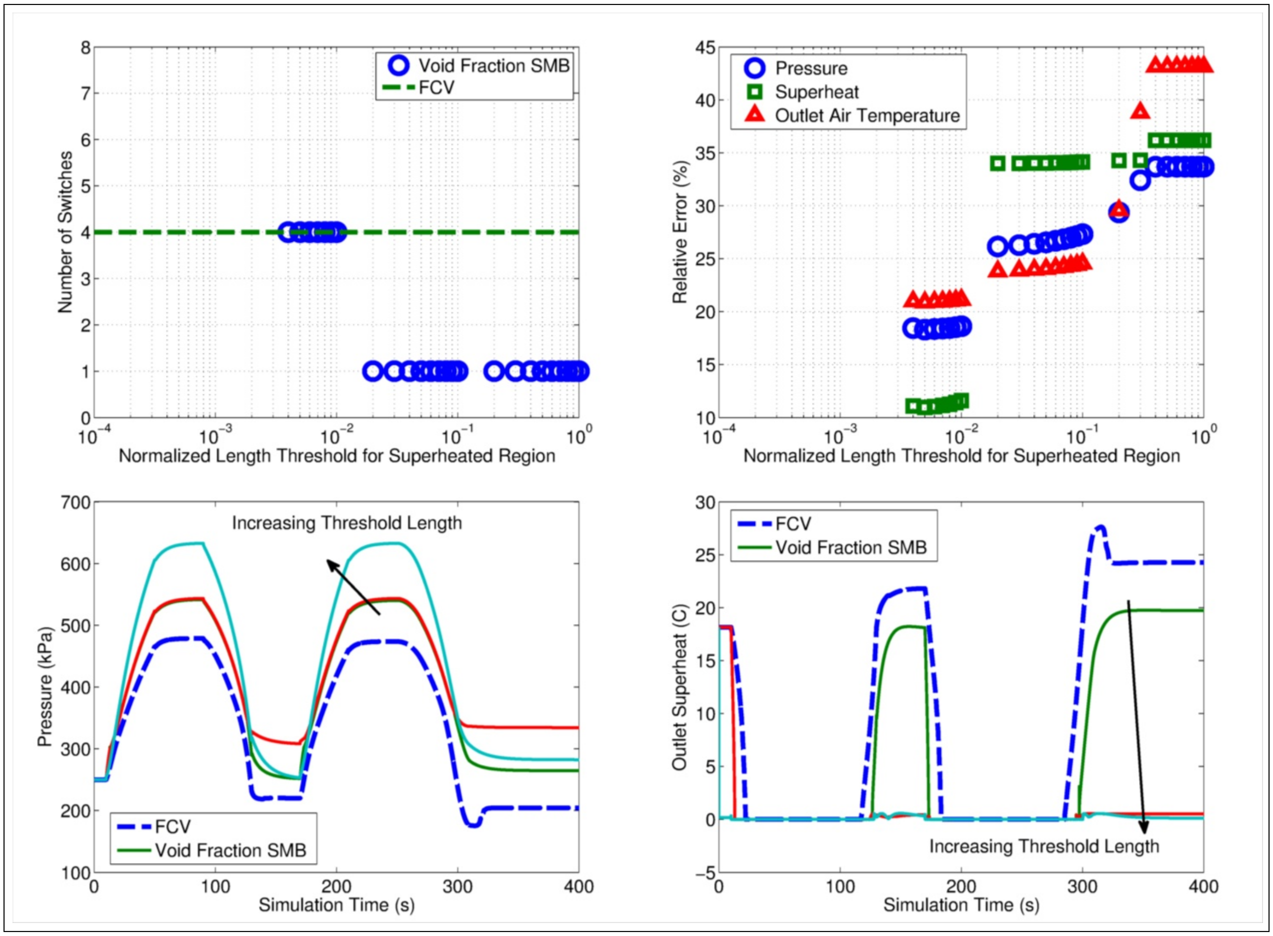

Fig. 14: Comparison of minimum normalized threshold length, l_{eps}, for void fraction based SMB model - Case 3a

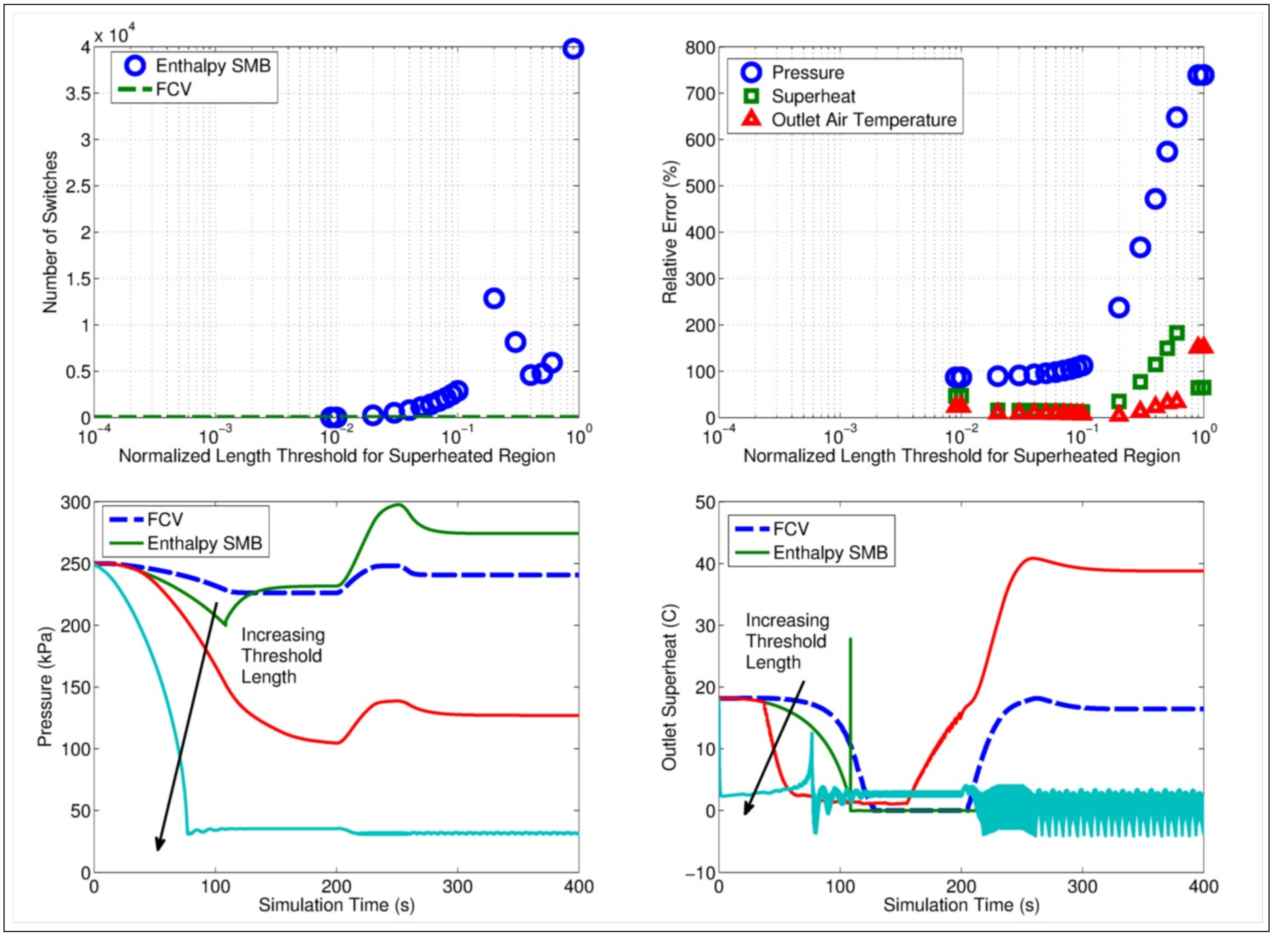

Fig. 15: Comparison of minimum normalized threshold length, l_{eps}, for enthalpy based SMB model - Case 3b

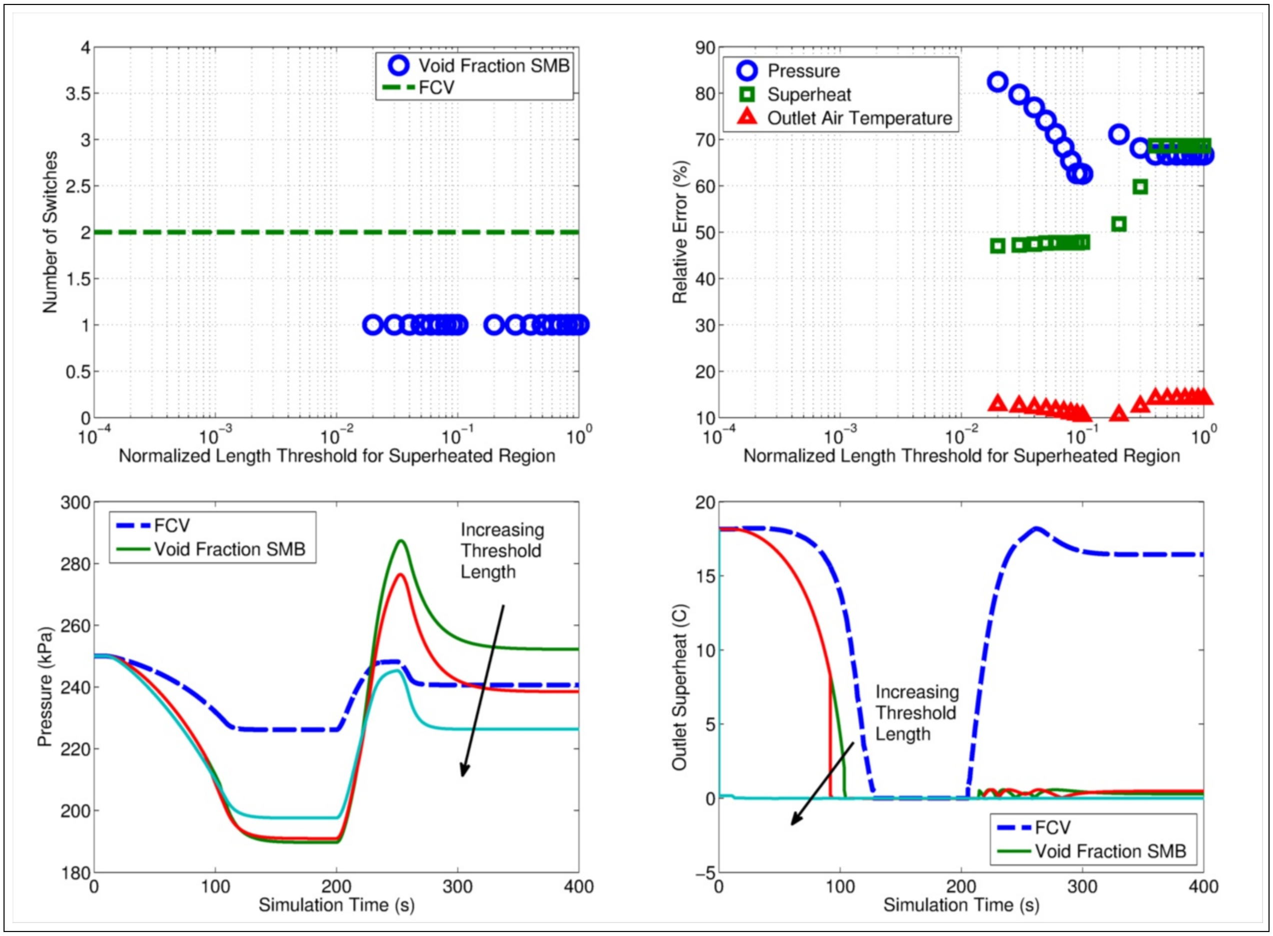

Fig. 16: Comparison of minimum normalized threshold length, l_{eps}, for void fraction based SMB model - Case 3b

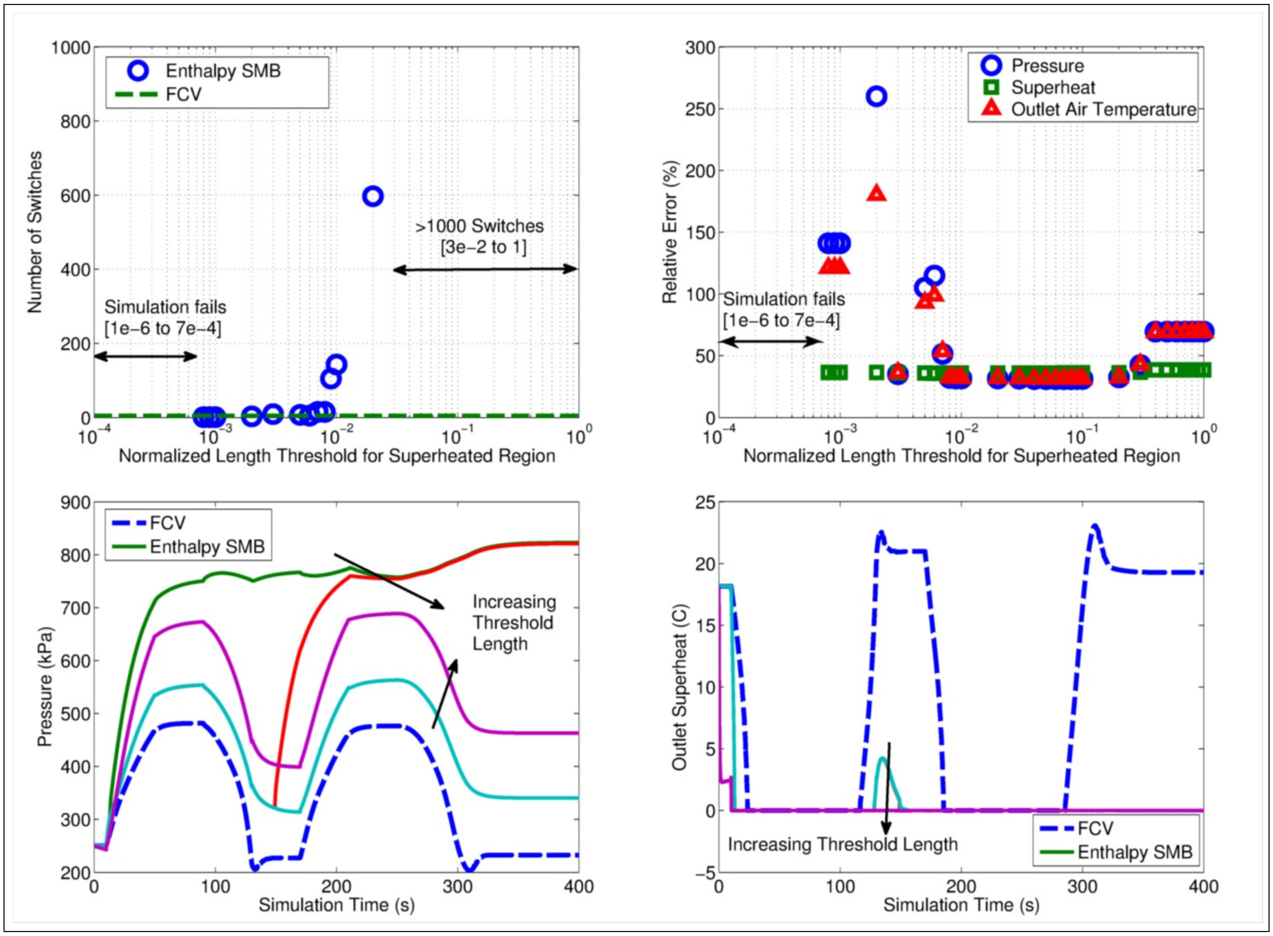

Fig. 17: Comparison of minimum normalized threshold length, l_{eps}, for enthalpy based SMB model - Case 3c

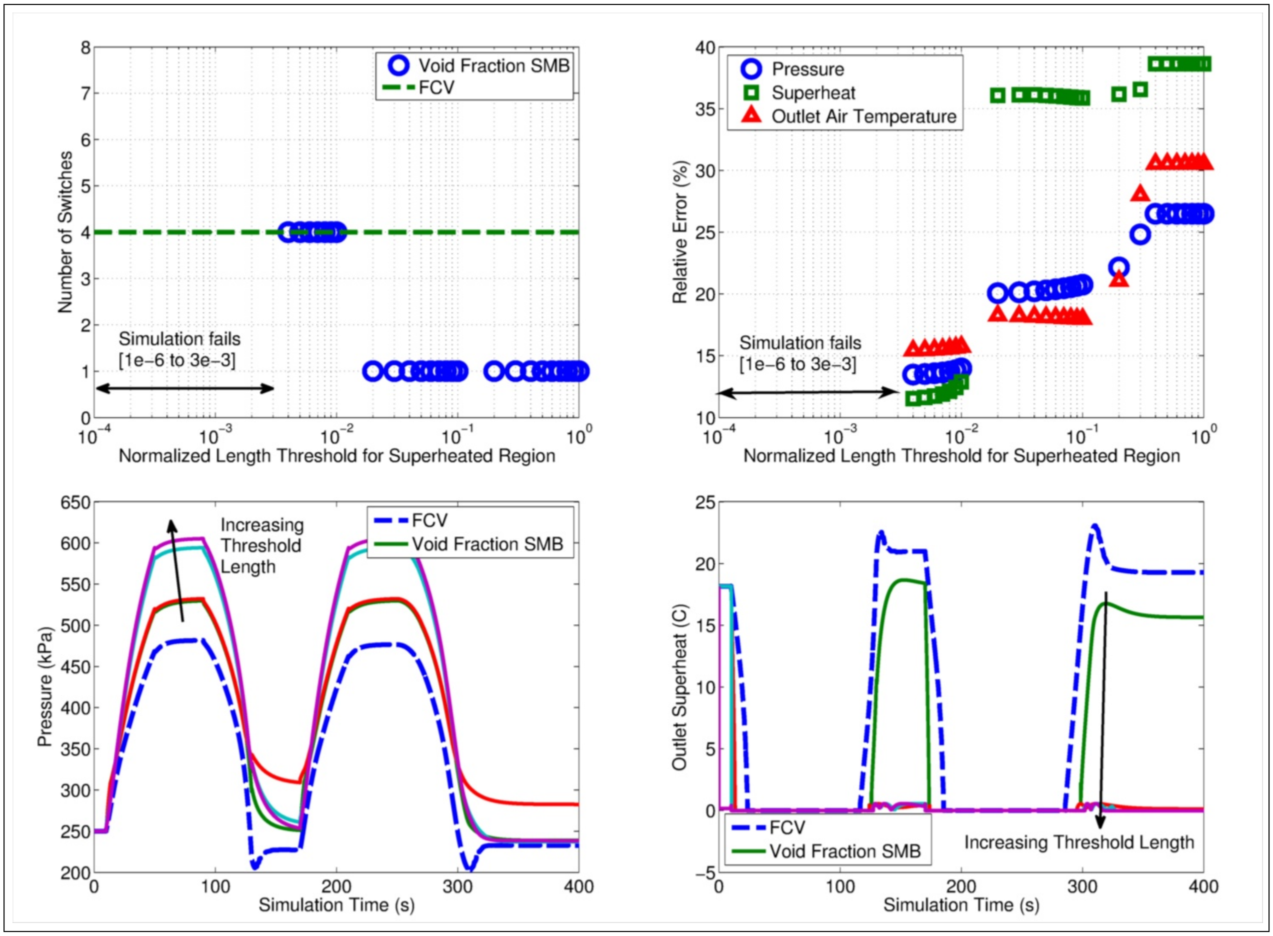

Fig. 18: Comparison of minimum normalized threshold length, l_{eps}, for void fraction based SMB model - Case 3c

B. Paradigm Comparison

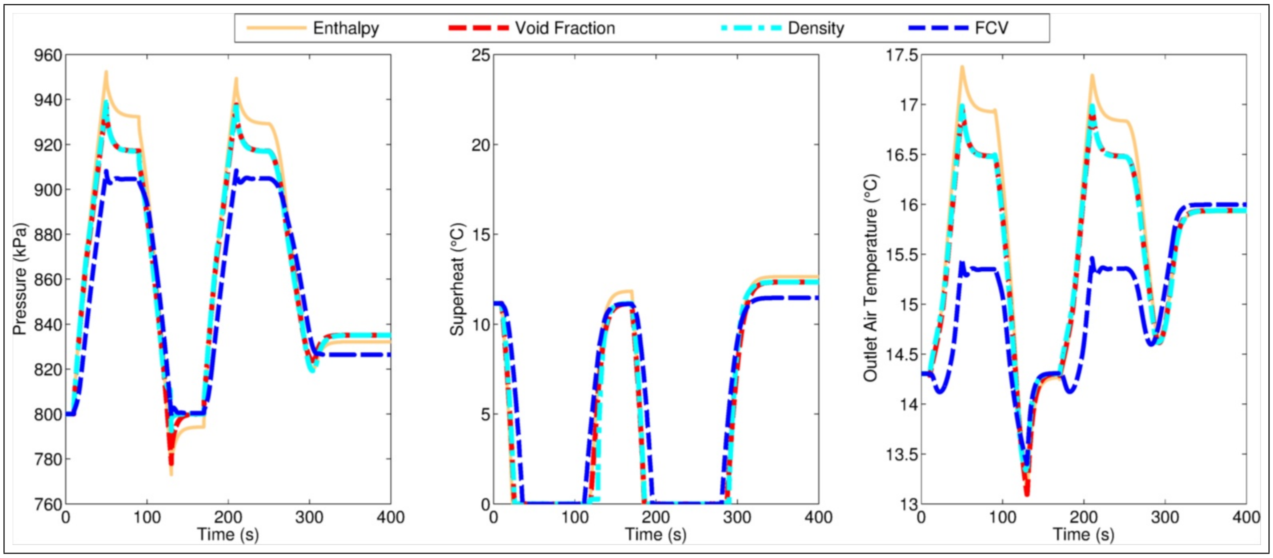

Fig. 19: Comparison of enthalpy SMB, void fraction SMB, density SMB, and FCV evaporator model outputs - Case 1a

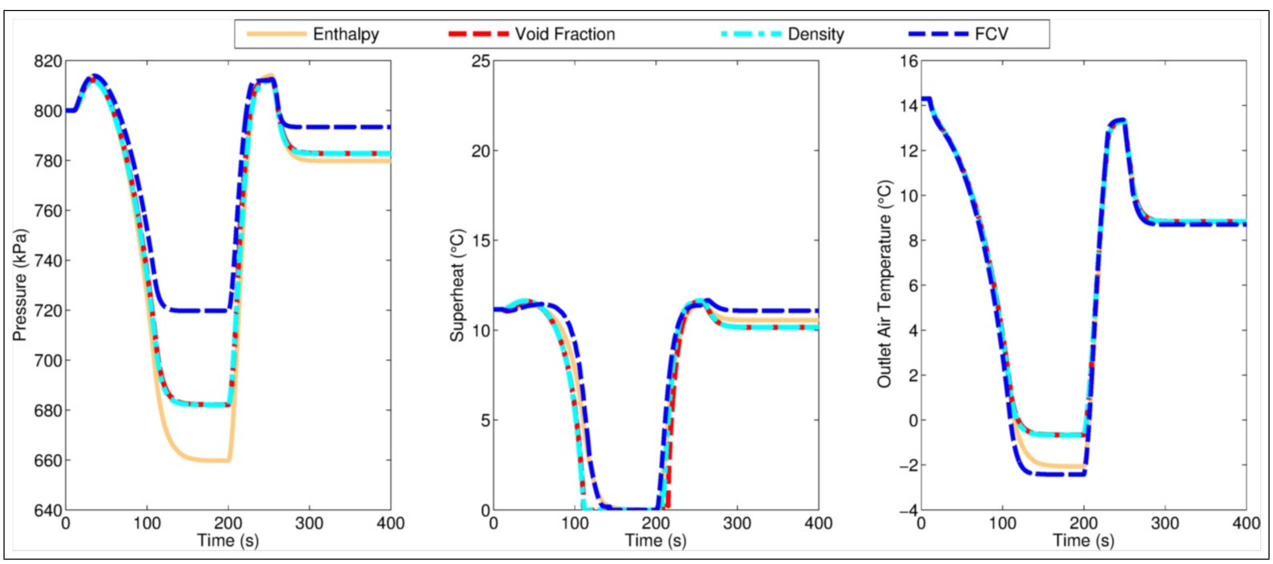

Fig. 20: Comparison of enthalpy SMB, void fraction SMB, density SMB, and FCV evaporator model outputs - Case 1b

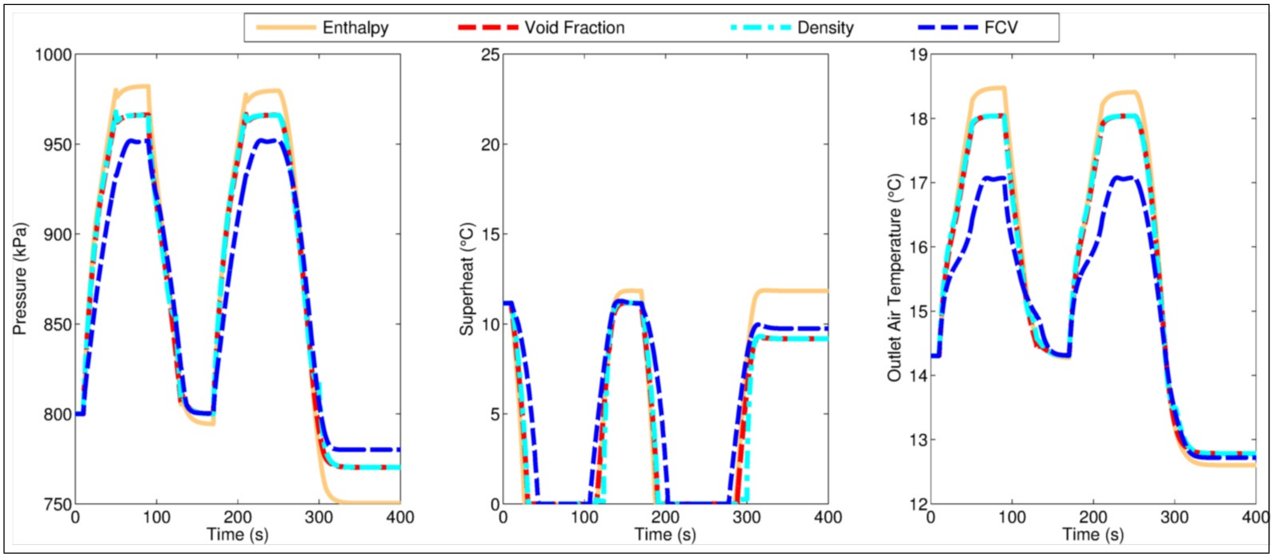

Fig. 21: Comparison of enthalpy SMB, void fraction SMB, density SMB, and FCV evaporator model outputs - Case 1c

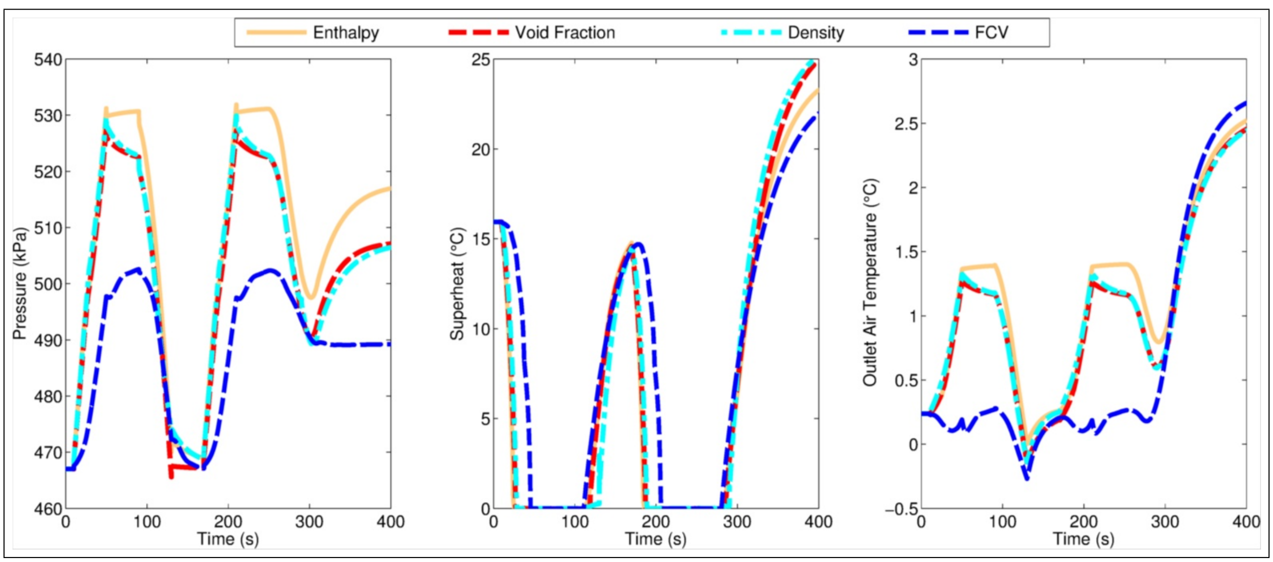

Fig. 22: Comparison of enthalpy SMB, void fraction SMB, density SMB, and FCV evaporator model outputs - Case 2a

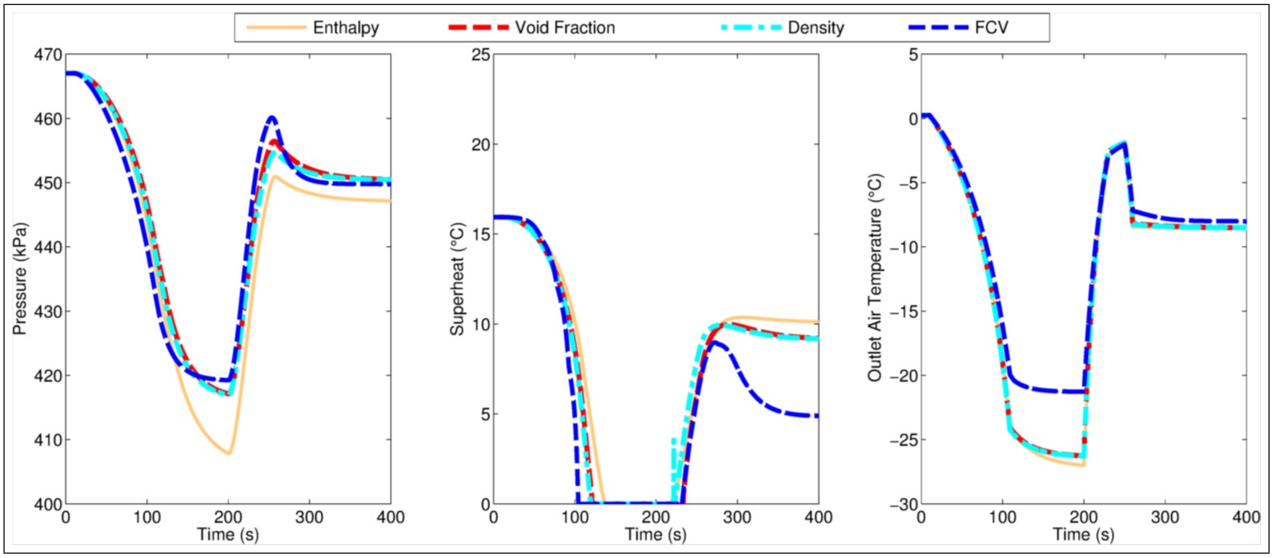

Fig. 23: Comparison of enthalpy SMB, void fraction SMB, density SMB, and FCV evaporator model outputs - Case 2b

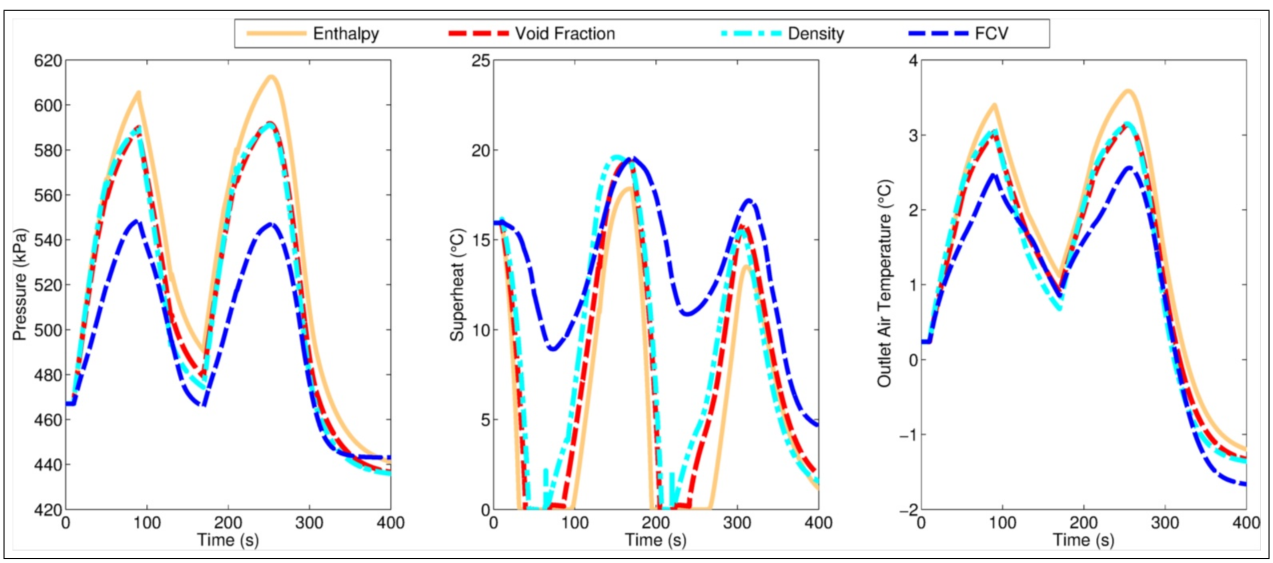

Fig. 24: Comparison of enthalpy SMB, void fraction SMB, density SMB, and FCV evaporator model outputs - Case 2c

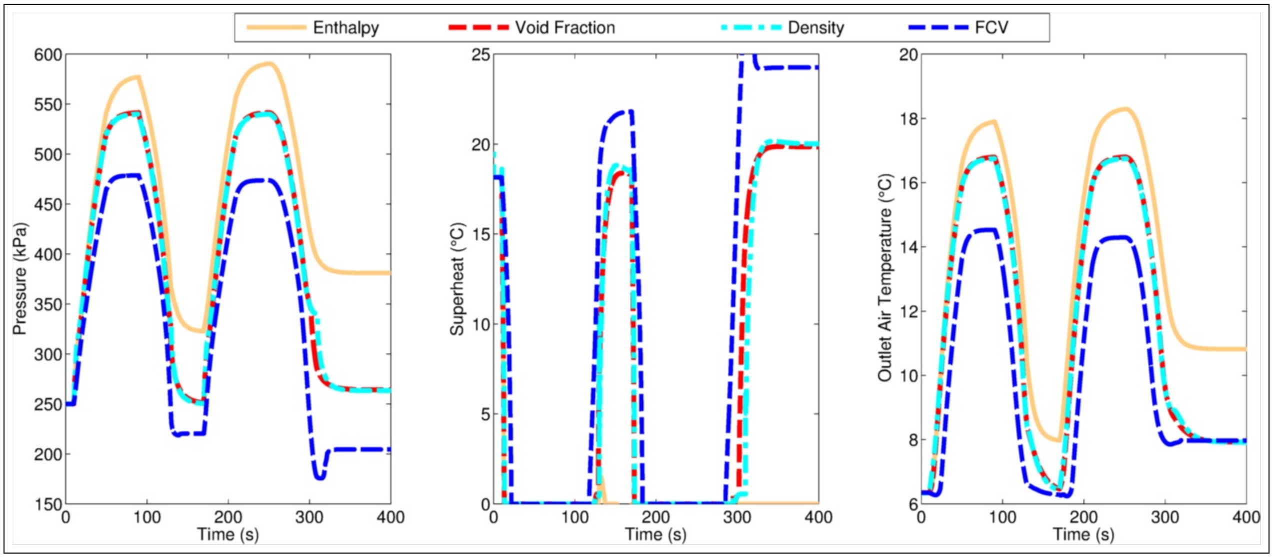

Fig. 25: Comparison of enthalpy SMB, void fraction SMB, density SMB, and FCV evaporator model outputs - Case 3a

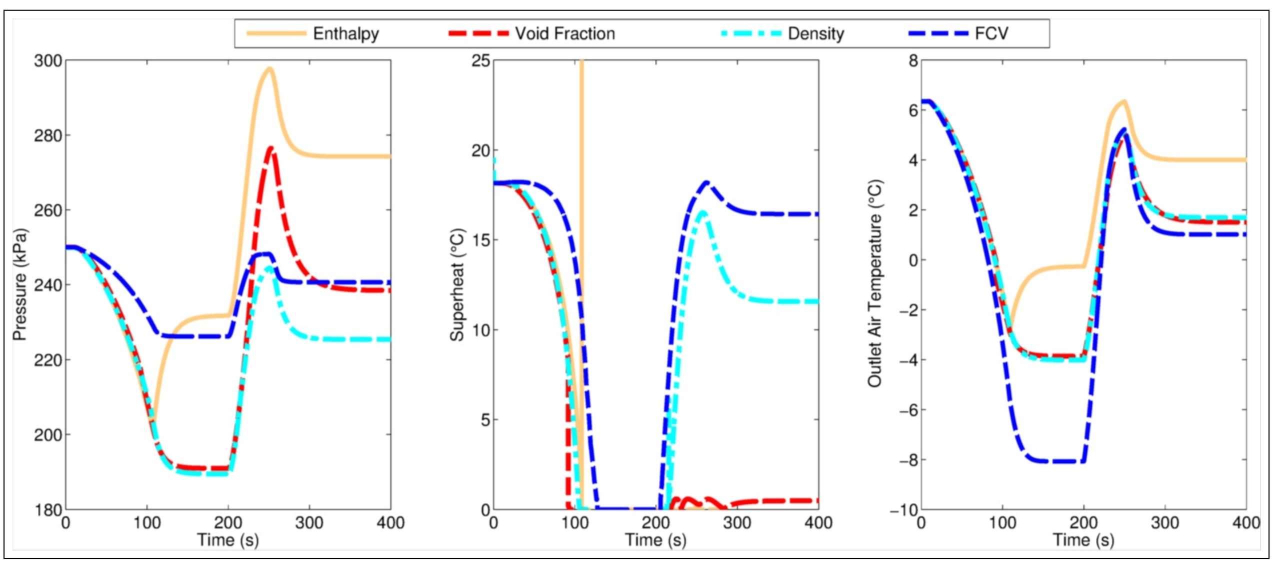

Fig. 26: Comparison of enthalpy SMB, void fraction SMB, density SMB, and FCV evaporator model outputs - Case 3b

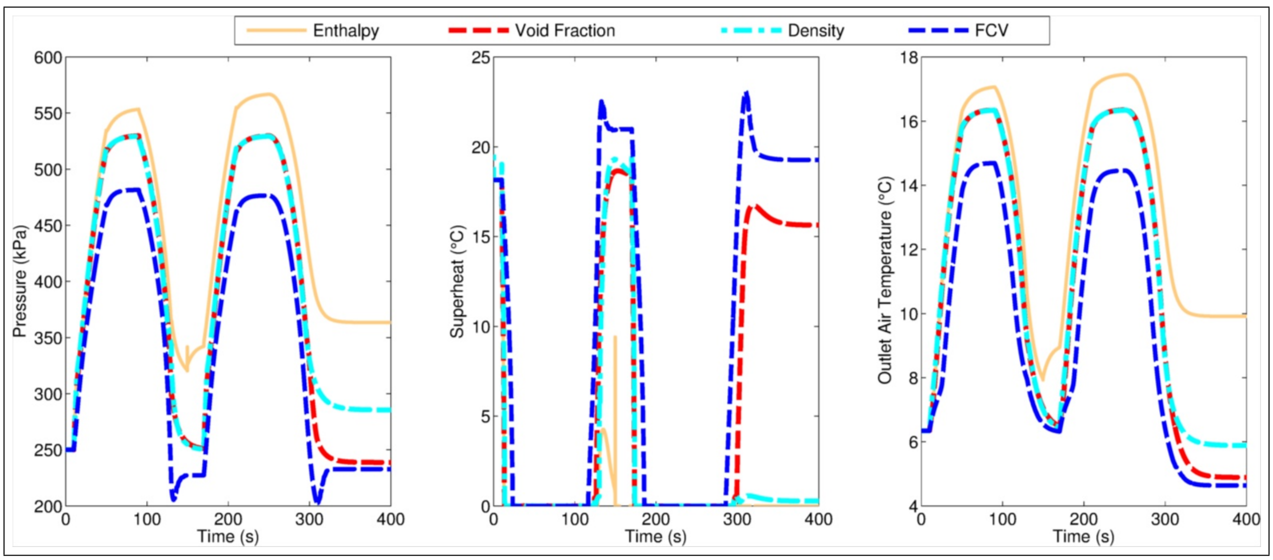

Fig. 27: Comparison of enthalpy SMB, void fraction SMB, density SMB, and FCV evaporator model outputs - Case 3c

REFERENCES

[1] Gnielinski, V. (1976). New equations for heat and mass-transfer in turbulent pipe and channel flow. *International Chemical Engineering*, 16(2), 359-368.

[2] Kays, W.M., and A.L. London, 1984. Compact heat exchangers. *McGraw-Hill Publishing, New York, NY*

[3] Wattelet, J.P. et al., 1994. Heat transfer flow regimes of refrigerants in a horizontal - tube evaporator. *ACRC TR-55, University of Illinois at Urbana-Champaign*